A lattice Boltzmann model for multiphase fluid flows

Daryl Grunau, Shiyi Chen, and Kenneth Eggert

Citation: Physics of Fluids A: Fluid Dynamics **5**, 2557 (1993); doi: 10.1063/1.858769
View online: http://dx.doi.org/10.1063/1.858769
View Table of Contents: http://aip.scitation.org/toc/pfa/5/10
Published by the American Institute of Physics

A lattice Boltzmann model for multiphase fluid flows

Daryl Grunau,[a),b)] Shiyi Chen,[b),c)] and Kenneth Eggert[a)]
Los Alamos National Laboratory, Los Alamos, New Mexico 87545

(Received 27 January 1993; accepted 24 May 1993)

A lattice Boltzmann equation method for simulating multiphase immiscible fluid flows with variation of density and viscosity, based on the model proposed by Gunstensen *et al.* for two-component immiscible fluids [Phys. Rev. A **43**, 4320 (1991)] is developed. The numerical measurements of surface tension and viscosity agree well with theoretical predictions. Several basic numerical tests, including spinodal decomposition, two-phase fluid flows in two-dimensional channels, and two-phase viscous fingering, are shown in agreement of experiments and analytical solutions.

I. INTRODUCTION

It has recently been shown that lattice gas computational fluid dynamics, including lattice gas automata (LGA)[1] and the lattice Boltzmann (LB)[2] equation methods, provide alternative numerical techniques for solving the Navier–Stokes equations, multiphase fluid flows,[3–5] and a variety of other fluid systems.[6,7] The parallel nature of these newly developed schemes, adapted from cellular automata, affords an easy implementation of fast, efficient, and accurate simulations on parallel machines.

To solve incompressible fluid flows by traditional numerical methods such as finite differences or finite elements, one must deal with a Poisson equation for the pressure term that is induced by the continuum condition and the momentum equation. Solution of the Poisson equation can be avoided by relaxing the incompressibility requirement, and penalizing errors in velocity divergence.[8] Lattice gas methods are most closely compared to these pseudocompressible algorithms for solving incompressible fluid flows. However, penalty of nonvanishing velocity gradients appear in the macroscopic equations as a result of microscopic particle dynamics. A lattice gas solver is only required to solve the kinetic equation of the particle distribution function. All other quantities, including density, velocity, and energy can be obtained by a macroscopic averaging process through the distribution function. Thus, the pressure effects on the momentum equation are controlled by an equation of state.

Since lattice gas algorithms proceed at a microscopic scale, compressible effects on the macroscopic fluid behavior can become significant. Nonetheless, the incompressible limit theory of lattice gas methods[9] and their numerical simulations,[7] predict and demonstrate that such a lattice gas solution at low Mach number produces results comparable with those of the incompressible Navier–Stokes equations for a wide variety of problems and with very small numerical errors. Also, two-phase surface dynamic boundaries and wall boundaries are far more easily implemented with a lattice gas method compared to direct simulations of the incompressible Navier–Stokes equations.[3,7]

Rothman and Keller[3] were the first to extend the single-phase lattice gas model proposed by Frisch, Hasslacher, and Pomeau (FHP)[1] to simulate multiphase fluid problems. Colored particles were introduced to distinguish between phases, and a nearest-neighbor particle interaction was used to facilitate interfacial dynamics, such as Laplace's formula for surface tension. Later, Somers and Rem[4] and Chen *et al.*[5] extended the original colored particle scheme by introducing colored holes. It has been shown[5] that the colored-hole lattice gas method extends the original nearest-neighbor particle interaction to several lattice lengths, leading to a Yukawa potential. Moreover, the colored-hole scheme carries purely local information in its particle collision step, reducing the size of the lookup table in the algorithm, and consequently speeding up the simulation.

Although two-phase lattice gas algorithms are able to produce interesting surface phenomena, they are difficult to compare quantitatively with experiments and other numerical simulations due to their noisy characteristics induced by particle fluctuations. The lattice Boltzmann model proposed by McNamara and Zanetti,[2] however, solves the kinetic equation for the particle *distribution* instead of tracking each particle's motion, as is done in lattice gas methods. Nonetheless, lattice gas algorithms will be superior to lattice Boltzmann models for simulating underlying physics and modeling microscopic dynamics, such as correlation effects and phase transitions, since they contain more information about the microscopic behavior of particles. On the other hand, to provide a numerical method for solving partial differential equations governing macroscopic behavior, lattice Boltzmann schemes will be at least as good as lattice gas models. The finite-difference nature of lattice Boltzmann methods not only can simulate the macroscopic equations more efficiently and accurately, but also preserve some of the advantages of lattice gas models, such as their parallel computing nature and their ease of boundary implementation.

Combining the lattice Boltzmann ideology of McNamara and Zanetti[2] with the linearized collision operator proposed by Higuera and Jimenez,[10] Gunstensen *et al.*[11] proposed a lattice Boltzmann method for solving two-phase fluid flows based on the Rothman and Keller lattice gas model.[3] An important contribution of this model is the

[a)]Earth and Environment Science Division.
[b)]Theoretical Division.
[c)]Center for Nonlinear Studies.

 0899-8213/93/5(10)/2557/6/$6.00

introduction of a perturbation step (shown in detail below) so that Laplace's formula at an interface can be approximately recovered. This lattice Boltzmann method has been used in several applications,[12] however, it has a few fundamental problems. First, the model does not solve the exact two-phase fluid equations—although Galilean invariance is recovered by the proper assignment of rest particles, the equation of state remains to be velocity dependent.[13] Second, the model uses a fully linearized collision operator, which involves a 24×24 matrix multiplication at each time step and position in three-dimensional space, reducing computational efficiency. Finally, the model does not include two-phase fluid flows that have variable densities and viscosities. In this paper, we extend their model by using a single-time relaxation lattice Boltzmann model. With the proper choice of the particle equilibrium distribution function, we are able to recover the incompressible Navier–Stokes equations for the color-blind fluid. In addition, our new model makes provision for variable densities and viscosities by use of the freedom of the rest particle equilibrium distribution, and a space-dependent relaxation process. For simplicity, we present a two-phase, two-dimensional fluid model on a hexagonal lattice in this paper. The extension of the current model to multiphase fluids and other lattices, including a two-dimensional square lattice, a three-dimensional face-centered hypercubic lattice,[9] and a body-centered-cubic[14] lattice, will be presented in detail in another paper.[15]

II. NUMERICAL MODEL

Denote $f_i(\mathbf{x},t)$, $f_i^{(r)}(\mathbf{x},t)$, and $f_i^{(b)}(\mathbf{x},t)$ as the particle distribution functions at space $\mathbf{x}$ and time t for total, red, and blue fluids, respectively. Here $i=0,1,\ldots,N$, where $N=6$ is the number of moving particle directions on a hexagonal lattice, and $f_i=f_i^{(r)}+f_i^{(b)}$. The lattice Boltzmann equation for both red and blue fluids can be written as follows:

$$f_i^k(\mathbf{x}+\mathbf{e}_i,t+1)=f_i^k(\mathbf{x},t)+\Omega_i^k(\mathbf{x},t), \tag{1}$$

where k denotes either the red or blue fluid and $\Omega_i^k=(\Omega_i^k)^1+(\Omega_i^k)^2$ is the collision operator. Note that in the two-phase lattice Boltzmann model by Gunstensen *et al.*, only a color-blind kinetic equation was given. The first term of the collision operator, $(\Omega_i^k)^1$, represents the process of relaxation to local equilibrium. For simplicity, we use a linearized collision operator with a single time relaxation parameter τ_k,[16,17]

$$(\Omega_i^k)^1=\frac{-1}{\tau_k}(f_i^k-f_i^{k(\mathrm{eq})}).$$

Here $f_i^{k(\mathrm{eq})}$ is the local equilibrium state depending on the local density and velocity, and τ_k is a spatially dependent characteristic relaxation time for species k. In lattice gas automaton models, the form of the local equilibrium state and rate of relaxation to the local equilibrium distribution are completely determined by the particle scattering process. From a statistical point of view, the macroscopic effects of these collisions only arise in the transport coefficients. Therefore, lattice Boltzmann models ignore particle collision details such as collision cross sections and frequencies. In addition, the local equilibrium state can be arbitrarily chosen,[13] with the exception that it must satisfy the conservation of mass and momentum:

$$\rho_r=\sum_i f_i^r=\sum_i f_i^{r(\mathrm{eq})},$$

$$\rho_b=\sum_i f_i^b=\sum_i f_i^{b(\mathrm{eq})},$$

and

$$\rho\mathbf{v}=\sum_{i,k} f_i^k\mathbf{e}_i=\sum_{i,k} f_i^{k(\mathrm{eq})}\mathbf{e}_i.$$

Here ρ_r and ρ_b are densities of the red and blue fluids, respectively, $\rho=\rho_r+\rho_b$ is the total density, and $\mathbf{v}$ is the local velocity.

Following the pressure-corrected Galilean-invariant single-phase lattice Boltzmann model proposed by Ref. 13, we assume the following equilibrium distribution for both red and blue fluids:

$$f_i^{r(\mathrm{eq})}=\rho_r\left(\frac{1}{6+m_r}+\frac{1}{3}(\mathbf{e}_i\cdot\mathbf{v})+\frac{2}{3}(\mathbf{e}_i\cdot\mathbf{v})^2-\frac{1}{6}v^2\right),$$

$$f_0^{r(\mathrm{eq})}=\rho_r\left(\frac{m_r}{6+m_r}-v^2\right),$$

$$f_i^{b(\mathrm{eq})}=\rho_b\left(\frac{1}{6+m_b}+\frac{1}{3}(\mathbf{e}_i\cdot\mathbf{v})+\frac{2}{3}(\mathbf{e}_i\cdot\mathbf{v})^2-\frac{1}{6}v^2\right),$$

$$f_0^{b(\mathrm{eq})}=\rho_b\left(\frac{m_b}{6+m_b}-v^2\right).$$

Here we have introduced two real-valued parameters, m_r and m_b. They can be understood as the ensemble-averaged number of degenerate rest particle states for the red and blue fluids, respectively. To achieve a stable interface, we furthermore assume that the moving particle distributions for both red and blue fluids are the same when $\mathbf{v}=0$:, i.e., $d=\rho_r/(6+m_r)=\rho_b/(6+m_b)$. This implies the following density ratio:

$$\gamma=\frac{\rho_r}{\rho_b}=\frac{6+m_r}{6+m_b}.$$

The second part of the collision operator is similar to that given in the Gunstensen *et al.* paper:

$$(\Omega_i^k)^2=(A_k/2)\,|\mathbf{F}|\,[(\mathbf{e}_i\cdot\mathbf{F})^2/|\mathbf{F}|^2-\tfrac{1}{2}],$$

where $\mathbf{F}$ is the local color gradient, defined as

$$\mathbf{F}(\mathbf{x})=\sum_i \mathbf{e}_i[\rho_r(\mathbf{x}+\mathbf{e}_i)-\rho_b(\mathbf{x}+\mathbf{e}_i)].$$

Note that in a single-phase region of our incompressible fluid model, $\mathbf{F}=0$. Thus the second term of the collision operator, $(\Omega_i^k)^2$, only has a contribution at two-phase interfaces. The parameter A_k is a free parameter, controlling the surface tension (shown below). For simplicity, we choose $A_r=A_b=A$ in this paper.

To maintain surfaces between fluids, we follow Rothman's scheme[3] to redistribute colored particles at two-phase interfaces (without changing the total particle distribution, f_i) by enforcing the red color momentum $\mathbf{j}^r=\Sigma_i f_i^r \mathbf{e}_i$, to align with the direction of the local color gradient. In other words, we redistribute the red density at an interface to maximize the following quantity: $-(\mathbf{j}^r\cdot\mathbf{F})$. The blue particle distribution can then be recovered using $f_i^b=f_i-f_i^r$.

To derive hydrodynamics, we use a long-wavelength, low-frequency approximation and a multiscaling analysis as follows:[18]

$$\frac{\partial}{\partial t}=\epsilon\frac{\partial}{\partial t_1}+\epsilon^2\frac{\partial}{\partial t_2}+\cdots,$$

$$\frac{\partial}{\partial x}=\epsilon\frac{\partial}{\partial x_1}.$$

Here t_1 and t_2 represent fast and slow time scales, respectively, and ϵ is assumed to be a small expansion parameter.

A Taylor series expansion of Eq. (1) to second order in the lattice spacing and time step gives the following continuum kinetic equation:

$$\frac{\partial f_i^k}{\partial t}+\mathbf{e}_i\cdot\nabla f_i^k+\frac{1}{2}\mathbf{e}_i\mathbf{e}_i:\nabla\nabla f_i^k+\mathbf{e}_i\cdot\nabla\frac{\partial}{\partial t}f_i^k+\frac{1}{2}\frac{\partial}{\partial t}\frac{\partial}{\partial t}f_i^k=\Omega_i^k. \tag{2}$$

Taking the zeroth- and first-order moments of $\mathbf{e}_i$ over Eq. (2), we readily obtain the continuum equations for the red and blue fluids, and the following momentum equation for the color-blind (total) fluid:

$$\frac{\partial(\rho v_\alpha)}{\partial t}+\frac{\partial}{\partial x_\beta}\sum_{i,k}(\mathbf{e}_i)_\alpha(\mathbf{e}_i)_\beta\left[f_i^{k(\mathrm{eq})}+\left(1-\frac{1}{2\tau_k}\right)f_i^{k(1)}\right]=0,$$

where $f_i^{k(1)}$ is the next-order perturbation for f_i^k and $(-1/2\tau_k)f_i^{k(1)}$ is attributed to the second-order components of (2). Note that since

$$\sum_i(\Omega_i^k)^2=\sum(\Omega_i^k)^2\mathbf{e}_i=0$$

and

$$\mathbf{F}=\tfrac{1}{3}\nabla(\rho_r-\rho_b)+\cdots\sim\epsilon+o(\epsilon^2),$$

the second term in the collision operator does not contribute to the continuum and momentum equations of the first-order approximation. It, however, will contribute to the pressure term at an interface: $P=P_0+\epsilon|\nabla F|$, where P_0 comes from the equation of state.

Our two-phase immiscible fluid model contains three fluid regions: a red or blue homogeneous region and a thin region, where the two fluids mix at the interfaces. In a homogeneous region, the evolution of our model will recover the Navier–Stokes equations with kinematic viscosity of $\nu_k=(2\tau_k-1)/8$ and a sound speed of $c_k=\sqrt{3/(6+m_k)}$ according to the Chapman–Enskog expansion shown in Ref. 14. A variation of viscosities for the two fluids can be obtained by choosing different τ_k.

The last issue remaining to be addressed is the interfacial dynamics that take place in a region where red and blue fluids are adjacent. Usually the thickness of such an interface will depend on an averaged relaxation time and the rest particle distribution. There are several ways to construct a relaxation parameter so that the red and blue fluids have a smooth change of viscosity at their interfaces. To do this, we define an order parameter, ψ, depending on red and blue densities as follows: $\psi=(\rho_r-\rho_b)/(\rho_r+\rho_b)$. Note that, in general, $|\psi|\leqslant 1$, however, in a purely red fluid region, $\psi=1$, and in a purely blue fluid region, $\psi=-1$. To continuously connect relaxation parameters τ_r and τ_b at an interface, we employ the following simple formula:

$$\tau=\begin{cases}\tau_r, & \psi>\delta,\\ g_r(\psi), & \delta\geqslant\psi>0,\\ g_b(\psi), & 0\geqslant\psi\geqslant-\delta,\\ \tau_b, & \psi<-\delta,\end{cases}$$

where $g_r(\psi)$ and $g_b(\psi)$ are second-order functions of ψ:

$$g_r(\psi)=\alpha+\beta\psi+\kappa\psi^2$$

and

$$g_b(\psi)=\alpha+\eta\psi+\xi\psi^2.$$

Assuming that $g_r(\delta)=\tau_r$, $g_b(-\delta)=\tau_b$, $\partial\tau/\partial\psi=0$ at $|\psi|=\delta$ and $g_r(0)=g_b(0)=\langle\tau\rangle$, we have $\alpha=2\tau_r\tau_b/(\tau_r+\tau_b)$, $\beta=2(\tau_r-\alpha)/\delta$, $\kappa=-\beta/(2\delta)$, $\eta=2(\alpha-\tau_b)/\delta$, and $\xi=\eta/(2\delta)$. Here $\delta\leqslant 1$ is a free parameter controlling the interface thickness and $\langle\tau\rangle$ is the averaged relaxation time step across the interface, $\langle\tau\rangle=2\tau_r\tau_b/(\tau_r+\tau_b)$.

Using the definition of mechanical surface tension given in Ref. 19,

$$\sigma=\int(P_n-P_t)dx, \tag{3}$$

and, after some algebra,[15] we obtain a theoretical formula for the surface tension on a two-dimensional hexagonal lattice: $\sigma=9A\langle\tau\rangle d(12+m_r+m_b)$. Here the integration is over whole space along the direction perpendicular to a given interface, and P_n and P_t are, respectively, the normal and tangential stress tensor at the two-phase interface. In Fig. 1, we show the theoretical prediction (—) and numerical measurements ($\diamondsuit$ and $+$) of σ as a function of particle density d with a mass ratio, $\gamma=\frac{8}{7}$. The $\diamondsuit$ symbols represent numerical measurements of surface tension using the above definition, and the $+$ signs represent the surface tension obtained by the Laplace formula $\Delta P=2\sigma/R$. The mechanical surface tension was obtained by numerical integration of (3) across an interface, whereas surface tension from Laplace's law was inferred from the slope of ΔP plotted against $1/R$ for radii ranging from 20 to 40. As can be seen, the theoretical prediction and numerical measurements agree very well in both cases.

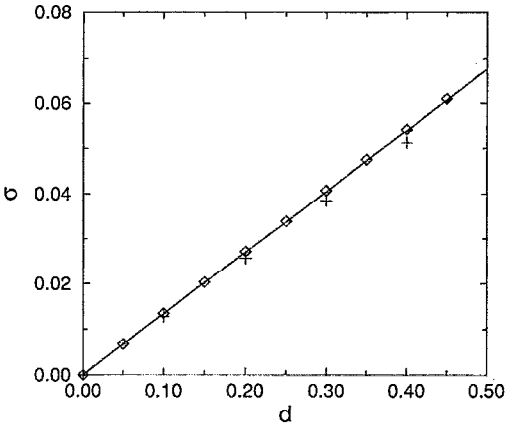

FIG. 1. The theoretical prediction (—) and numerical measurements (◇ and +) of surface tension σ as a function of particle density d with a mass ratio $\gamma=\frac{8}{7}$.

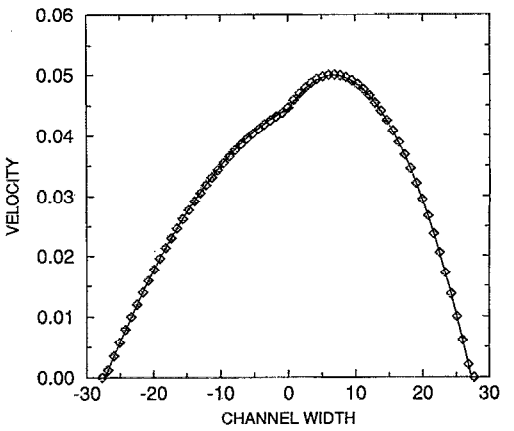

FIG. 3. The analytical prediction (—) and direct numerical simulation (◇) of velocity as a function of channel width y.

III. NUMERICAL SIMULATIONS AND DISCUSSION

To demonstrate the application of the presented lattice Boltzmann model, we show three numerical examples below. The first numerical test is the study of the phase segregation process by two-dimensional spinodal decomposition when the fluids have differing densities. Figure 2 is a snapshot ($t=8300$) of the two-phase area distribution, when the density ratio, $\gamma=\rho_r/\rho_b$, is 2.3. One can see that the red fluid (shown as black) represents a high-density region and the blue fluid (shown as white) represents a low-density region. The initial condition for this simulation is constant density and random color distribution with periodic boundaries. Here the surface tension parameter is set to $A=0.01$. The current model preserves the basic two-phase segregation processes and, in simulations not shown here, we have seen the preservation of stable two-phase interfaces for much higher density ratios (~ 200). This capability will allow us to approach the simulation of gas and oil mixing flows.

The second numerical test is two-dimensional channel flow with two fluids having different viscosities. A lattice length of 65 in the y direction ($W=65$) and 128 in the x direction ($L=128$) is used, with a nonslip condition on both the upper and bottom boundaries. Initially, the lower half space (from lattice 1–32) is filled with red fluid, and the top half space (from lattice 34–65) is filled with blue fluid. The middle line is initialized to half red and half blue, and the relaxation parameters for red and blue fluids are assigned values of $\tau_r=2$ and $\tau_b=1$. Using the viscosity formula discussed above, this translates into a kinematic viscosity ratio of 3:1 for the red and blue fluids, respectively. A forcing technique, as described in Ref. 13, is used to establish a small pressure gradient across the length of the channel. Assuming a thin interface in the middle, an analytical solution of the velocity distribution as a function of the channel width, y, can be derived, centered on the middle of the channel:[20]

$$v_x^r=\frac{(P_0-P_L)w^2}{2\mu_r L}\left(\frac{2\mu_r}{\mu_r+\mu_b}+\frac{\mu_r-\mu_b}{\mu_r+\mu_b}\frac{y}{w}-\frac{y^2}{w}\right),$$

$$v_x^b=\frac{(P_0-P_L)w^2}{2\mu_b L}\left(\frac{2\mu_b}{\mu_r+\mu_b}+\frac{\mu_r-\mu_b}{\mu_r+\mu_b}\frac{y}{w}-\frac{y^2}{w}\right),$$

where $(P_0-P_L)/L$ is the pressure gradient across the channel, μ_r and μ_b are shear viscosities for red (0.7875) and blue (0.2625) fluids, respectively. Here, also, $w=\sqrt{3}W/4$ is half the channel width, where the factor $\sqrt{3}/2$ is a hexagonal lattice effect. In Fig. 3 we present the analytical prediction (—) and direct numerical simulation (◇) for velocity as a function of channel width y. As seen, the agreement is excellent.

The last numerical test is a two-dimensional Hele–Shaw viscous fingering experiment. The upper and lower walls are assigned a no-slip boundary condition, and the fluids are given a viscosity ratio of 1:10 by assigning $\tau_r=1$ and $\tau_b=5.5$. To develop a Hele–Shaw pattern, an initial perturbation is introduced at the interface,[21,22] which is then forced by maintaining a high pressure at the inlet and low pressure at the outlet. The shape of the finger can be altered by a change in the surface tension parameter A, given as 0.0065 in this experiment. Figure 4 shows the evolution of a less viscous fluid penetrating one having a higher viscosity at times=0, 2000, 4000, 6000, 8000, and

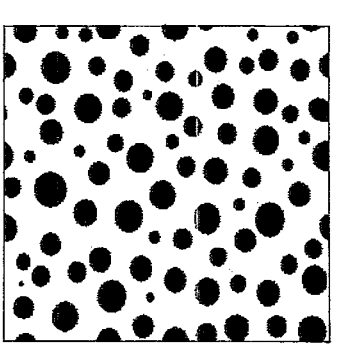

FIG. 2. A snapshot at time $t=8300$ of the area density distribution of a spinodal decomposition simulation, where the two fluids have a 2.3:1 mass ratio, γ. The boundaries are periodic, and the initial red and blue density is assigned a common constant value, with a random color distribution. The surface tension parameter is assigned to $A=0.01$.

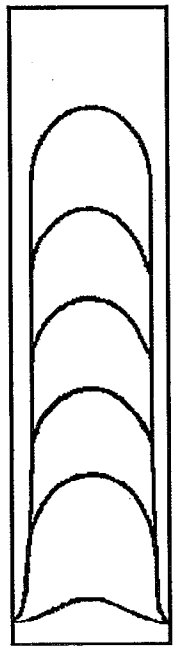

FIG. 4. The formation of a stable finger in a Hele–Shaw cell at times $t=0$, 2000, 4000, 6000, 8000, and 10 000. A viscosity ratio of 1:10 is established by setting $\tau_r=1$ and $\tau_b=5.5$. The low-viscosity fluid is penetrating the higher-viscosity region.

10 000. We see that a stable finger develops and is maintained throughout the simulation, although we expect a tip-splitting instability to occur for smaller values of A, as demonstrated by Ref. 22. This phenomenon will be discussed in more detail in a subsequent paper. The fluid patterns shown here are similar to results obtained by other numerical methods.[22]

The lattice Boltzmann model in this paper is the extension of the model proposed by Gunstensen *et al.* The current model gives an exact Navier–Stokes solution, in the incompressible limit, for each fluid individually. The surface tension at an interface satisfies the Laplace formula, and the model has the capability to simulate two-phase fluid flows with different densities and viscosities. The simulation results for several typical two-phase fluid flows are shown, in good agreement, with analytical solutions and some experimental observations. Several issues, however, remain to be addressed. First, to achieve a density variation, the current model uses the freedom of the rest particle equilibrium distribution. Although the scheme is simple, it is difficult to obtain high velocity flows, since the assignment of a high particle mass ratio will accumulate a large number of particles in the rest state, reducing the fluid speed. In addition, the equation of state of the current model is that of an ideal gas similar to the original FHP model. To simulate fluid flows with a large density variation, a lattice Boltzmann model with an equation of state for nonideal gases (liquids) may provide some alternatives. Second, the current model uses two parabolic curves to match the interface relaxation characteristic time in the mixing region. For a very thin interface (for example, one lattice width), the effects of the parameter δ will be negligible. On the other hand, for flows with slow relaxation, the interface will be much wider. The relaxation form and the choice of δ may affect interfacial dynamics. Other functional forms, such as a binormal distribution, may give better results.

ACKNOWLEDGMENTS

We thank R. Vaidya, G. D. Doolen, and H. Chen for useful suggestions. Eugene Loh is a contributor of the original CM-2 code.

This work is performed under the auspices of the United States Department of Energy, by Los Alamos National Laboratory, under Contract No. W-7405-ENG-36. Numerical simulations were carried out using the computational resources at the Advanced Computing Laboratory at Los Alamos. Partial funding for this work was provided by the Oil Recovery Technology Partnership under the U.S. Department of Energy Office of Fossil Energy, administered by the Bartlesville Project Office.

[1] U. Frisch, B. Hasslacher, and Y. Pomeau, "Lattice-gas automata for the Navier–Stokes equation," Phys. Rev. Lett. **56**, 1505 (1986).
[2] G. G. McNamara and G. Zanetti, "Use of the Boltzmann equation to simulate lattice-gas automata," Phys. Rev. Lett. **61**, 2332 (1988); F. J. Higuera, S. Succi, and R. Benzi, "Lattice gas dynamics with enhanced collisions," Europhys. Lett. **9**, 345 (1989).
[3] D. H. Rothman and J. M. Keller, "Immiscible cellular-automaton fluids," J. Stat. Phys., **52**, 1119 (1988).
[4] J. A. Somers and P. C. Rem, "Analysis of surface tension in two-phase lattice gases," Physica D **47**, 39 (1991).
[5] S. Chen, G. D. Doolen, K. Eggert, D. Grunau, and E. Y. Loh, "Local lattice-gas model for immiscible fluids," Phys. Rev. A **43**, 7053 (1991).
[6] G. D. Doolen, in *Lattice Gas Methods for PDE's* (Addison–Wesley, Reading, MA, 1989); G. D. Doolen, "Lattice gas methods for PDE's: Theory, applications and hardware," Physica D **47**, No. 1 & 2 (1991).
[7] S. Chen, G. D. Doolen, and W. H. Matthaeus, "Lattice gas automata for simple and complex fluids," J. Stat. Phys. **64**, 1133 (1991); R. Kapral, A. Lawniczak, and P. Masiar, "Oscillations and waves in a reactive lattice-gas automaton," Phys. Rev Lett. **66**, 2539 (1991).
[8] J. D. Ramshaw and G. L. Mesina, "A hybrid penalty-pseudocompressibility method for transient incompressible fluid flow," Comput. Fluids **20**, 165 (1991).
[9] U. Frisch, D. d'Humières, B. Hasslacher, P. Lallemand, Y. Pomeau, and J. P. Rivet, "Lattice gas hydrodynamics in two and three dimensions," Complex Syst. **1**, 649 (1987).
[10] F. Higuera and J. Jimènez, "Boltzmann approach to lattice gas simulations," Europhys. Lett. **9**, 663 (1989).
[11] A. K. Gunstensen, D. H. Rothman, S. Zaleski, and G. Zanetti, "Lattice Boltzmann model of immiscible fluids," Phys. Rev. A **43**, 4320 (1991).
[12] A. K. Gunstensen, Ph.D. dissertation, 1992.
[13] H. Chen, S. Chen, and W. H. Matthaeus, "Recovery of the Navier–Stokes equations using a lattice gas Boltzmann method," Phys. Rev. A **45**, R5339 (1991).
[14] S. Chen, J. Wang, X. Shan, and G. Doolen, "Lattice Boltzmann computational fluid dynamics in three dimensions," J. Stat. Phys. **68**, 379 (1992).
[15] D. Grunau, S. Chen, K. Eggert, and G. Doolen (in preparation).
[16] S. Y. Chen, H. D. Chen, D. Martinez, and W. Matthaeus, "Lattice Boltzmann model for simulation of magnetohydrodynamics," Phys. Rev. Lett. **67**, 3776 (1991).
[17] Y. H. Qian and P. Lallemand, "Lattice BGK models for Navier–Stokes equation," Europhys. Lett. **17**, 479 (1992).

[18]F. J. Alexander, S. Chen, and J. D. Sterling, "Lattice Boltzmann thermohydrodynamics," Phys. Rev. E. **47**, R2279 (1993).
[19]J. Rowlinson and B. Widom, *Molecular Theory of Capillarity* (Clarendon, Oxford, 1982).
[20]R. B. Bird, W. E. Stewart, and E. N. Lightfoot, *Transport Phenomena* (Wiley, New York, 1960).
[21]D. Burgess and F. Hayot, "Saffman-Taylor-type instability in a lattice gas," Phys. Rev. A **40**, 5187 (1989); E. Meilburg and G. M. Homsy, "Nonlinear unstable viscous fingers in Hele–Shaw flows. II. Numerical simulation," Phys. Fluids **31**, 429 (1988).
[22]A. J. DeGregoria and L. W. Schwartz, "A boundary-integral method for two-phase displacement in Hele–Shaw cells," J. Fluid Mech. **164**, 383 (1986).